Materials Views

FULL PAPER

Quinacridone-Based Electron Transport Layers for Enhanced Performance in Bulk-Heterojunction Solar Cells

Toan V. Pho, Heejoo Kim, Jung Hwa Seo, Alan J. Heeger, and Fred Wudl*

A water/alcohol-soluble small molecule based on the commercially available pigment quinacridone is employed as an electron transport layer in organic photovoltaics. The quinacridone derivative is utilized in solution-processed bulk-heterojunction solar cells to improve primarily the fill factor of the devices, contributing to an upwards of 19% enhancement in the power conversion efficiency relative to the control devices with no electron transport layer. The facile synthesis of the quinacridone derivative coupled with the ease of device fabrication via solution processing provide a simple, yet effective means of improving the performance of existing organic photovoltaic cells.

1. Introduction

Organic photovoltaics (OPVs) have emerged as a promising technology for low-cost, large-area solar energy conversion,[1] but the low efficiencies relative to their inorganic counterparts remain a cause for concern. Recent efforts at enhancing device performance have focused on improving the collection of charge carriers, particularly through modification of the electrical contacts.[2] At the cathode interface, the use of low work function metals such as Ca has been found to dramatically improve the performance of OPVs due to the enhancement of the internal electric field.[3] However, the oxidative instability of these metals is detrimental to device lifetimes, and hence, expensive encapsulation processes are generally required to provide protection from ambient conditions.[4] While cathodes consisting of higher work function metals such as Al are more stable, these metals incur a smaller voltage offset with the anode material, which results in a reduced built-in electric field that can inhibit the transport of charge carriers and thus increase the propensity for charge recombination. To alleviate these concerns, the addition of an electron transport layer (ETL) between the active layer and cathode can facilitate electron transport to the cathode. However, the use of an ETL complicates the solution processing of multilayered OPV devices, as solvents of orthogonal polarity for each successive layer are needed to prevent removal of the underlying layers, thereby necessitating the development of ETL materials that are water/alcohol-soluble.

To this end, water/alcohol-soluble polymers such as poly(ethylene oxide)[5] or conjugated polyelectrolytes[6] have been previously utilized as ETLs in OPVs. The efficacy of these materials, however, is constrained by disadvantages inherent to all polymers - namely, batch-to-batch variations in terms of polydispersity and molecular weight as well as difficulties in purification and characterization. Additional difficulties are encountered with other water/alcohol-processable electron transport materials such as zinc oxide (ZnO) nanoparticles[7] or titanium suboxide (TiO_x).[8] The synthesis of ZnO nanoparticles often encounters issues with controlling size distribution and reproducibility, whereas the microstructure of TiO_x is highly dependent on post-deposition cross-linking,[8b,9] potentially inducing structural variations from batch-to-batch.

In light of these developments, water/alcohol-soluble small molecules for ETLs are a simpler, more attractive alternative to their polymeric and inorganic counterparts. A newly discovered group of water-soluble small molecules based on the commercially available pigment quinacridone has been shown to significantly reduce the electron injection barrier in organic light-emitting diodes (OLEDs).[10] Given the apparent advantages in OLEDs, we evaluated the applicability of the easily accessible quinacridone material ($Na^+QHSO_3^-$, **Figure 1**a) as an ETL in OPVs.

T. V. Pho, Dr. H. Kim,[+] Dr. J. H. Seo,[++] Prof. A. J. Heeger, Prof. F. Wudl
Department of Chemistry and Biochemistry & Center for Polymers and Organic Solids
University of California, Santa Barbara
E-mail: wudl@chem.ucsb.edu
[+] Present address: Heeger Center for Advanced Materials, Gwangju Institute of Science and Technology, South Korea
[++] Present address: Department of Materials Physics, Dong-A University, South Korea

2. Device Fabrication

OPVs were fabricated according to the device architecture (Figure 1c): indium tin oxide (ITO)/poly(3,4-ethylenedioxythiophene):poly(styrenesulfonate) (PEDOT:PSS)/active layer/$Na^+QHSO_3^-$-based ETL/Al. The bulk-heterojunction active layer consisting of $PCDTBT:PC_{71}BM$ (1:4, w/w) or $Si-PCPDTBT:PC_{71}BM$ (1:4, w/w) was deposited on top of the PEDOT:PSS from *o*-dichlorobenzene:chlorobenzene or chlorobenzene solution, respectively. $PC_{71}BM$ is [6,6]-phenyl C_{71} butyric acid methyl ester, and the structures of poly[*N*-9'-heptadecanyl-2,7-carbazole-*alt*-5,5-(4',7'-di-2-thienyl-2',1',3'-benzothiadiazole)] (PCDTBT)[11]

www.MaterialsViews.com

ADVANCED
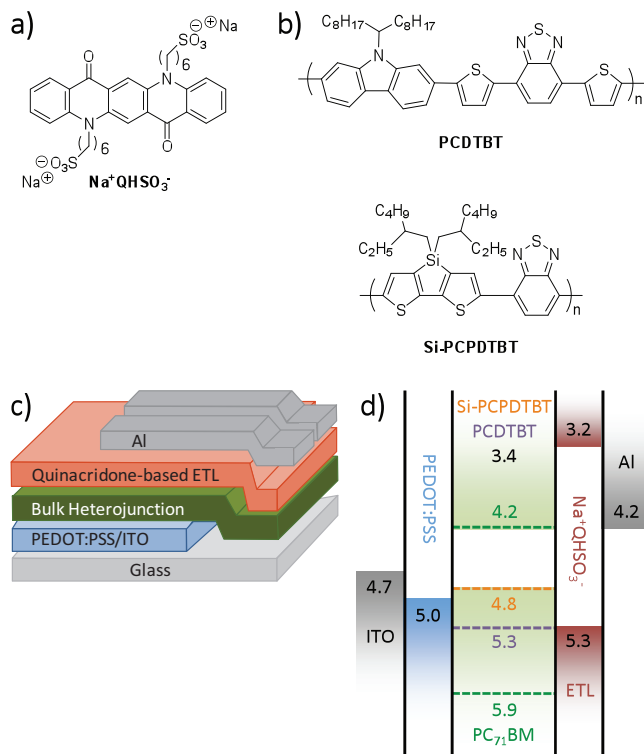FUNCTIONAL
MATERIALS
www.afm-journal.de

FULL PAPER

Figure 1. a) Molecular structure of the ETL material. b) Donor polymers used in the bulk heterojunction layers. c) Device architecture. d) Energy level diagram of the solar cell materials.

Figure 2. Device performance of OPVs with and without the $Na^+QHSO_3^-$-based ETL.

and poly[(4,4′-bis(2-ethylhexyl)dithieno[3,2-*b*:2′,3′-*d*]silole)-2,6-diyl-*alt*-(2,1,3-benzothiadiazole)-4,7-diyl] (Si-PCPDTBT)[12] are shown in Figure 1b. To avoid perturbation of the active layer, the quinacridone-based ETL ($Na^+QHSO_3^-$) was deposited from methanol. Control devices without a layer of the quinacridone derivative were also fabricated for comparison.

3. Results and Discussion

Current density–voltage (*J–V*) characteristics of an initial set of solar cells are shown in **Figure 2**. The short circuit current (J_{sc}), open circuit voltage (V_{oc}), fill factor (*FF*), and power conversion efficiency (PCE) were calculated from the *J–V* curves and are summarized in **Table 1**. The addition of the ETL to the PCDTBT:PC_{71}BM devices resulted in a significant increase in the FF, contributing to an overall improvement in the PCE from 4.3% to 5.2%. Just as for PCDTBT:PC_{71}BM, the $Na^+QHSO_3^-$-based ETL demonstrated improvements with a different active layer material in Si-PCPDTBT:PC_{71}BM solar cells, raising the PCE from 2.9 to 3.2%. The use of the ETL enhanced the FF of the devices and had a negligible impact on the V_{oc} and J_{sc}.

The enhancement in FF was further investigated by varying the thickness of the ETL in PCDTBT:PC_{71}BM devices (**Figure 3**). The thicknesses of the ETLs were estimated to be smaller than 5 nm. Thus, the ETLs were, in
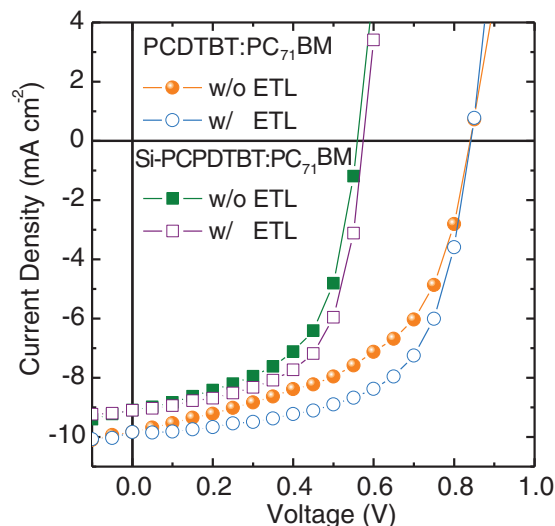
fact, too thin to be measured accurately by surface profilometry. Nevertheless, an improvement in FF was observed with the introduction of ETLs that were spin-cast at 1000 through 4000 rpm. Very thin ETLs (5000 rpm) contributed to a decrease in FF. This drop in performance may be attributed to dewetting of the very thin hydrophilic layer of the quinacridone derivative atop the hydrophobic bulk-heterojunction surface, resulting in a discontinuous ETL.

Analysis of the dark *J–V* characteristics of the devices (**Figure 4**) revealed significant suppression of the leakage and reverse currents (under low forward and reverse bias, respectively) relative to the control devices, indicative of improved diode characteristics. Indeed, with the addition of the ETL, the shunt resistance (R_{sh}) increased by approximately a factor of 5, whereas the series resistance (R_s) remained nearly the same (Table 1).

Since the enhancement in OPV performance may be correlated to more facile charge transport, organic field-effect transistors (OFETs) were fabricated to assess the impact of the ETL on the charge transport properties of the bulk-heterojunction. To best emulate the structure of the solar cells, the active layer in the OFETs was chosen to be Si-PCPDTBT:PC_{71}BM topped with the $Na^+QHSO_3^-$-based ETL (**Figure 5**a). Al source and drain electrodes were employed to mirror the Al cathode used in the OPVs. Control devices without the ETL were also fabricated to evaluate the mobility of the pristine bulk-heterojunction. With the insertion of the ETL, the electron mobility of the OFETs more than doubled from 1.8×10^{-3} to 3.8×10^{-3} cm^2 V^{-1} s^{-1}

Table 1. Summary of device performance of OPVs.

		J_{sc} [mA cm^{-2}]	V_{oc} [V]	FF [%]	PCE [%]	R_{sh} [Ω·cm^2]	R_s [Ω·cm^2]
PCDTBT:PC_{71}BM/Al	w/o ETL	9.83	0.84	52.6	4.34	9.78×10^2	0.47
	w/ETL	9.83	0.84	62.6	5.17	4.60×10^3	0.32
Si-PCPDTBT:PC_{71}BM/Al	w/o ETL	9.10	0.56	56.9	2.89	6.47×10^2	2.01
	w/ETL	9.10	0.57	61.9	3.23	3.65×10^3	1.91

**ADVANCED
FUNCTIONAL
MATERIALS**

www.afm-journal.de

Materials Views

www.MaterialsViews.com
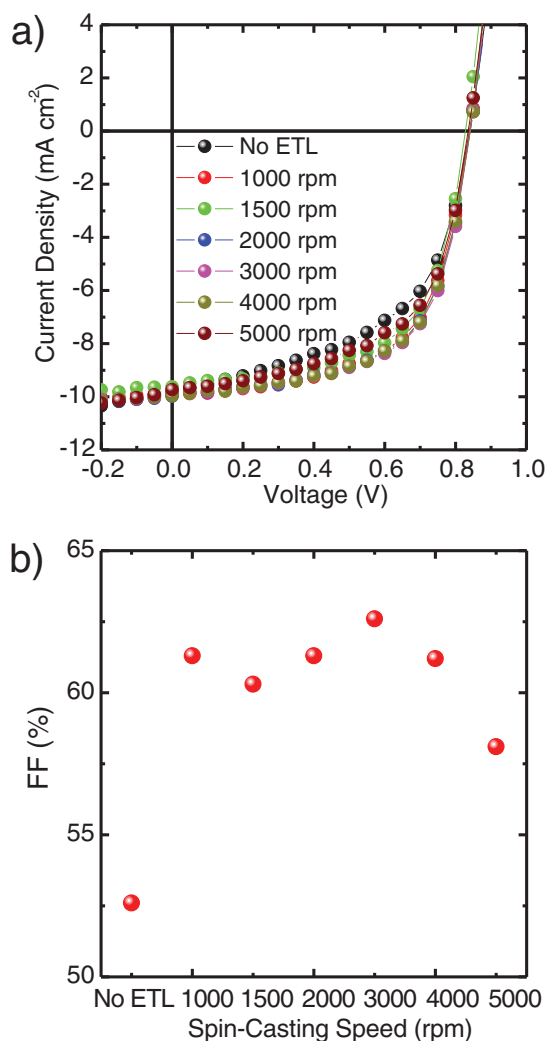
Figure 3. *J–V* (a) and FF (b) characteristics of PCDTBT:PC$_{71}$BM devices with different ETL thicknesses.

Figure 4. Dark *J–V* characteristics of the devices.

in diode characteristics. Notably, the Na$^+$QHSO$_3^-$-based ETL improved the FF despite the relatively high-lying LUMO (lowest unoccupied molecular orbital), which is aligned with neither

Figure 5. a) Device architecture of OFETs containing a Si:PCPDTBT:PC$_{71}$BM/ETL active layer. b) Transfer characteristics of the devices in *n*-channel operation mode with and without the ETL.

(Figure 5b), suggesting that the performance enhancement with the OPVs may be ascribable in part to the improved *n*-type transport. In contrast, the hole mobility remained relatively constant: 5.5×10^{-4} and 5.7×10^{-4} cm^2 V^{-1} s^{-1} with and without the ETL, respectively (data not shown). It should be noted that the hole mobilities are relatively low for Si-PCPDTBT-based systems[12b] because of the large contact resistance and injection barrier with the Al electrodes.

Although the electron transporting behavior of conjugated polyelectrolytes in OLEDs is typically ascribed to the involvement of an interfacial dipole[13] and/or ion motion,[14] it is unclear at this stage how those mechanisms would apply to the observed FF enhancement in OPVs. Conjugated polyelectrolytes have previously been utilized as ETLs in OPVs,[6] but the dearth of consistent interpretations and analyses further compounds our difficulty in ascertaining the theoretical underpinnings of the Na$^+$QHSO$_3^-$-based ETL. Nevertheless, the empirical data show that the addition of the ETL enhances the performance of OPVs, evident by the increase in FF and an improvement
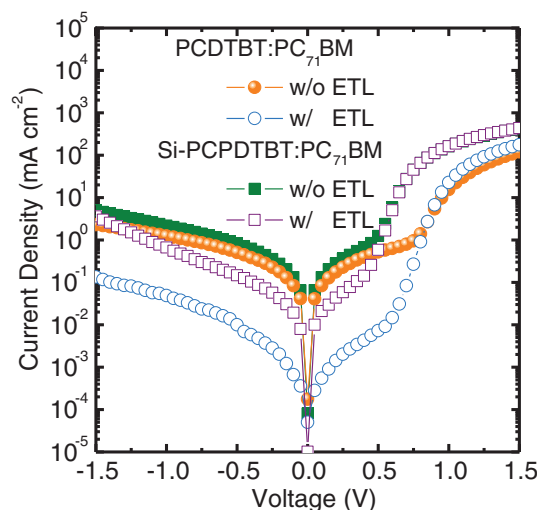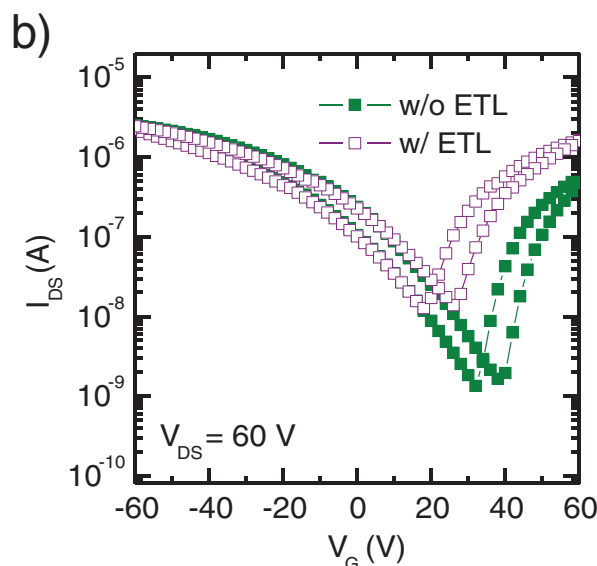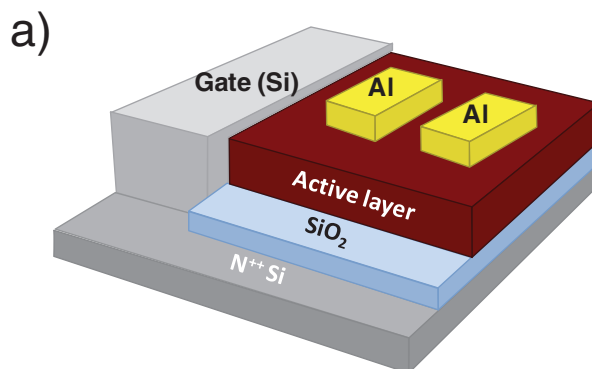
www.MaterialsViews.com

ADVANCED
FUNCTIONAL
MATERIALS
www.afm-journal.de

FULL PAPER

the LUMO of PC$_{71}$BM nor the work function of the Al cathode (Figure 1d). In addition, the enhancement in performance ostensibly does not arise from an intrinsic hole-blocking feature of the ETL, considering that the quinacridone derivative exhibits a HOMO (highest occupied molecular orbital) level higher than that of PC$_{71}$BM.

While the use of conjugated polyelectrolyte-based ETLs has been correlated primarily to an increase in V_{oc},[6a,6c] we observed little-to-no change in the V_{oc} with the addition of our small molecule Na$^+$QHSO$_3^-$-based ETL. It is currently unknown if the discrepancy in improvements is a function of the difference in conjugated motifs (fluorene in the conjugated polyelectrolytes vs. quinacridone in this work) and/or in the pendant ionic groups (cationic tetraalkylammonium vs. anionic alkylsulfonate). Nonetheless, the promising improvements with the FF and PCE warrant further investigation.

4. Conclusions

In summary, the simple application of a solution-deposited, small molecule ETL can improve the PCE of OPVs, obviating the need for post-deposition treatments such as cross-linking. Although the use of TiO$_x$ as an ETL in PCDTBT:PC$_{71}$BM solar cells yields a PCE of 6%,[8b] the addition of the quinacridone-based ETL does improve the device efficiency from 4.3% to 5.2%. The ETL also enhanced the performance of Si-PCPDTBT:PC$_{71}$BM solar cells, albeit to a lesser degree. In both cases, however, the overall enhancements in PCE are primarily derived from significant increases in the FF.

5. Experimental Section

OPV Fabrication: The quinacridone ETL material (Na$^+$QHSO$_3^-$) was prepared according to the literature procedure.[10] Bulk-heterojunction solar cells were fabricated on indium tin oxide (ITO) coated glass substrates. Poly(3,4-ethylenedioxythiophene):poly(styrenesulfonate) (PEDOT:PSS) was spin-coated in air from aqueous solution at 5000 rpm for 40 s onto the pre-cleaned ITO/glass to form a 40 nm thick film. The substrate was subsequently dried for 10 min at 140 °C and then transferred into a N$_2$ filled glove box. The blend solutions of PCPDTBT:PC$_{71}$BM (1:4 w/w) and Si-PCPDTBT:PC$_{71}$BM (1:4 w/w) were prepared in co-solvents of *o*-dichlorobenzene:chlorobenzene (3:1 v/v) and *o*-dichlorobenzene, respectively. The concentrations of the blend solutions were 7 mg (for the polymers) and 28 mg (for PC$_{71}$BM) per mL of solvent. The solutions of PCDTBT:PC$_{71}$BM (1:4) and Si-PCPDTBT:PC$_{71}$BM (1:4) were spin-casted at 5000 rpm for 40 s and 2000 rpm for 40 s, respectively, atop the PEDOT:PSS layers. The thicknesses of the PCDTBT:PC$_{71}$BM and Si-PCPDTBT:PC$_{71}$BM layers were 80 nm and 100 nm, respectively. The devices were subsequently annealed for 10 min at 80 °C. The quinacridone-based ETL (Na$^+$QHSO$_3^-$) solution (1 mg/10 mL in methanol) was then deposited on top of the active layer at 3000 rpm for 40 s. The devices were heated at 70 °C for 5 min in a N$_2$ filled glove box. Finally, Al metal was deposited by thermal evaporation in a vacuum of about 4×10^{-6} mbar.

OPV Characterization: Current-density–voltage (*J–V*) characteristic curves were measured using a Keithley 2400 source meter. Solar cell performance was measured using an Air Mass 1.5 Global solar simulator (100 mW cm^{-2}). An aperture (9.84 mm^2) was used on top of the cell to eliminate extrinsic effects such as cross talk, wave guiding, and shadow effect. All measurements were carried out under a N$_2$ atmosphere.

OFET Fabrication: Field-effect transistors were fabricated on heavily doped *n*-type Si wafers covered with a thermally grown 200 nm thick SiO$_2$

layer. The active layer consisting of Si-PCPDTBT:PC$_{71}$BM (1:4, w/w) was deposited from a 0.5 wt% solution in *o*-dichlorobenzene at 2000 rpm for 40 s. The ETL was then deposited from methanol solution at 4000 rpm. Al source and drain electrodes were deposited by thermal evaporation. The channel width and length were 50 μm and 1000 μm, respectively.

[1] G. Dennler, M. C. Scharber, C. J. Brabec, *Adv. Mater.* **2009**, *21*, 1323.

[2] a) H. Ma, H.-L. Yip, F. Huang, A. K. Y. Jen, *Adv. Funct. Mater.* **2010**, *20*, 1371; b) C. J. Brabec, S. E. Shaheen, C. Winder, N. S. Sariciftci, P. Denk, *Appl. Phys. Lett.* **2002**, *80*, 1288.

[3] a) V. D. Mihailetchi, L. J. A. Koster, P. W. M. Blom, *Appl. Phys. Lett.* **2004**, *85*, 970; b) P. W. M. Blom, V. D. Mihailetchi, L. J. A. Koster, D. E. Markov, *Adv. Mater.* **2007**, *19*, 1551.

[4] M. Jørgensen, K. Norrman, F. C. Krebs, *Sol. Energy Mater. Sol. Cells* **2008**, *92*, 686.

[5] F. Zhang, M. Ceder, O. Inganäs, *Adv. Mater.* **2007**, *19*, 1835.

[6] a) J. Luo, H. Wu, C. He, A. Li, W. Yang, Y. Cao, *Appl. Phys. Lett.* **2009**, *95*, 043301; b) S.-I. Na, S.-H. Oh, S.-S. Kim, D.-Y. Kim, *Org. Electron* **2009**, *10*, 496; c) C. He, C. Zhong, H. Wu, R. Yang, W. Yang, F. Huang, G. C. Bazan, Y. Cao, *J. Mater. Chem.* **2010**, *20*, 2617; d) S.-H. Oh, S.-I. Na, J. Jo, B. Lim, D. Vak, D.-Y. Kim, *Adv. Funct. Mater.* **2010**, *20*, 1977.

[7] H.-L. Yip, S. K. Hau, N. S. Baek, H. Ma, A. K. Y. Jen, *Adv. Mater.* **2008**, *20*, 2376.

[8] a) A. Hayakawa, O. Yoshikawa, T. Fujieda, K. Uehara, S. Yoshikawa, *Appl. Phys. Lett.* **2007**, *90*, 163517; b) S. H. Park, A. Roy, S. Beaupre, S. Cho, N. Coates, J. S. Moon, D. Moses, M. Leclerc, K. Lee, A. J. Heeger, *Nat. Photon.* **2009**, *3*, 297.

[9] J. Y. Kim, S. H. Kim, H. H. Lee, K. Lee, W. Ma, X. Gong, A. J. Heeger, *Adv. Mater.* **2006**, *18*, 572.

[10] T. V. Pho, P. Zalar, A. Garcia, T.-Q. Nguyen, F. Wudl, *Chem. Commun.* **2010**, *46*, 8210.

[11] a) N. Blouin, A. Michaud, M. Leclerc, *Adv. Mater.* **2007**, *19*, 2295; b) J. H. Seo, S. Cho, M. Leclerc, A. J. Heeger, *Chem. Phys. Lett.* **2011**, *503*, 101.

[12] a) M. C. Scharber, M. Koppe, J. Gao, F. Cordella, M. A. Loi, P. Denk, M. Morana, H.-J. Egelhaaf, K. Forberich, G. Dennler, R. Gaudiana, D. Waller, Z. Zhu, X. Shi, C. J. Brabec, *Adv. Mater.* **2010**, *22*, 367; b) M. Morana, H. Azimi, G. Dennler, H.-J. Egelhaaf, M. Scharber, K. Forberich, J. Hauch, R. Gaudiana, D. Waller, Z. Zhu, K. Hingerl, S. S. van Bavel, J. Loos, C. J. Brabec, *Adv. Funct. Mater.* **2010**, *20*, 1180; c) H. Kim, J. H. Seo, E. Y. Park, T.-D. Kim, K. Lee, K.-S. Lee, S. Cho, A. J. Heeger, *Appl. Phys. Lett.* **2010**, *97*, 193309.

[13] W. L. Ma, P. K. Iyer, X. Gong, B. Liu, D. Moses, G. C. Bazan, A. J. Heeger, *Adv. Mater.* **2005**, *17*, 274.

[14] a) C. V. Hoven, R. Yang, A. Garcia, V. Crockett, A. J. Heeger, G. C. Bazan, T.-Q. Nguyen, *Proc. Natl. Acad. Sci. USA* **2008**, *105*, 12730; b) H. Li, Y. Xu, C. V. Hoven, C. Li, J. H. Seo, G. C. Bazan, *J. Am. Chem. Soc.* **2009**, *131*, 8903; c) J. H. Seo, A. Gutacker, B. Walker, S. Cho, A. Garcia, R. Yang, T.-Q. Nguyen, A. J. Heeger, G. C. Bazan, *J. Amer. Chem. Soc.* **2009**, *131*, 18220.